CONCRETE RESEARCH LETTERS

www.crl.issres.net Vol. 6 (3) – Sept. 2015

Employing New Innovative Material for Airfield Pavement

A.A. Elsayed[1], and T. Sleem[2]

[1] *Associate Professor, Civil Engineering, Modern Academy for Engineering and Technology, Cairo, Egypt*

[2] *Civil Engineering, Modern Academy for Engineering and Technology, Cairo, Egypt*

Abstract

The main objective of this paper was to investigate the effect of horizontal force on the behavior of airfield pavement and new reinforced concrete slab during aircraft ground operation. In addition, the effects of various aircraft's wheel load configurations on the predicted airfield pavement life were discussed. To achieve these objectives, theoretical analysis, using the finite element (FE) programs SAP2000 and (ADINA) were performed. The maximum surface deflection, the maximum horizontal tensile strain (ε_t) at the bottom of asphalt concrete (AC) layer and the maximum compressive strain (ε_c) at the top of subgrade are the most commonly used criteria for flexible pavement design and they are used in this study as the basis of measuring the flexible pavement response. The research plan includes studying different sections of airfield pavements, where different AC layer thickness and different AC module were used. Based on the work of this study, modulus of elasticity, E_1 had a significant effect on the flexible pavement response and the predicted pavement life and there are three forces acting on the pavement through the tire: 1) longitudinal force (LGF), which is the tractive or breaking force, 2) lateral force (LTF) and 3) vertical wheel load (VL) which also affect the pavement response and predicted pavement life. It is shown in this study that the new reinforced concrete slab gives better results.

KEY WORDS

Flexible Pavements; Innovative Material; Structural Analysis; Finite element; ADINA

1. INTRODUCTION

A number of researchers studied the effect of E_1 on the flexible pavements behavior under VWL only. For example, Yue *et al.* [18] studied the flexible pavement response under different tire-pavement contact pressures. They found that, ε_t decreased as E_1 increased, however in cases of high-strength bases there was a critical E_1 value below which ε_t also decreased.

For the design procedure of pavement to be completely rational in nature, consideration should be given to all forces acting on airplane wheel. There are three forces acting on the pavement through the tire: 1) longitudinal force (LGF), which is the tractive or breaking force, 2) lateral force (LTF) and 3) vertical wheel load sections (VL). Horizontal forces are the great importance especially critical runway such as exits, entrances, and stop lines (sections of take-off operation). The main objective of this study was to identify the effect of such horizontal forces on the expected flexible airfield pavement behavior and the predicted pavement life under various wheel loads. Finite Element (FE) computer program SAP2000 was utilized to perform FE analysis throughout the work completed in this study. A Cartesian coordinate system was used, where the x and y axes represented the longitudinal and transverse directions of the pavement respectively, while the z-axis represented pavement depth. The positive direction of the y-axis is the traffic direction. The origin of the Cartesian coordinates is located at the corner of the model under the AC layer. Figure 1 and Figure 2 show a plan and isometric views for the FE model. The flexible pavement structure was assumed to have three layers (AC, untreated base, and subgrade). The interface between any two consecutive layers was assumed to be perfectly bonded as recommended by the Asphalt Institute [1].

SAP2000 is a FE structural analysis program deals with linear elastic materials. It has static analysis and dynamic analysis options. Element generation options are also available for convenience. Undeformed and deformed shape plotting capabilities exists for data verification of the model geometry and for studying the structural behavior of the system. All necessary geometric and loading options associated with the elements have been incorporated. The sensitivity analysis was focused on the effect of horizontal forces on the maximum surface deflection, the maximum tensile strain at the bottom of the AC layer, and the maximum compressive strain at the top of subgrade. They are the most commonly used criteria for flexible pavement design [6, 8, 15], and they were used in this paper as the basis for measuring the flexible pavement behavior under various aircraft wheel loads. Stresses and surface deflections were obtained directly from the SAP2000 solution phase. So, strains were calculated from the relationships of isotropic materials that assumed in this study. Allowable number of load repetitions based on fatigue cracking criteria (N_f) and allowable number of load repetitions to control permanent deformation (N_d) were calculated from the Asphalt Institute's equations

Numerical analysis has become an essential tool in investigating the soil structure interaction problems. One of the most powerful of numerical and versatile numerical analysis tools is the finite element method. It is capable of representing the structure, soil nonlinearity, non-homogeneity, and different soil layer and damping properties [11]. ADINA (Automatic Dynamic Incremental Nonlinear Analysis) is a FE structural analysis program deals with nonlinear materials. It has static analysis and dynamic analysis options. Element generation options are also available for convenience. ADINA method is one of the most powerful numerical techniques available today for the analysis of complex structural and mechanical systems. It is also proposed by several codes as an acceptable method of structural analysis. Figure 3, shows problem definition of soil structure interaction.

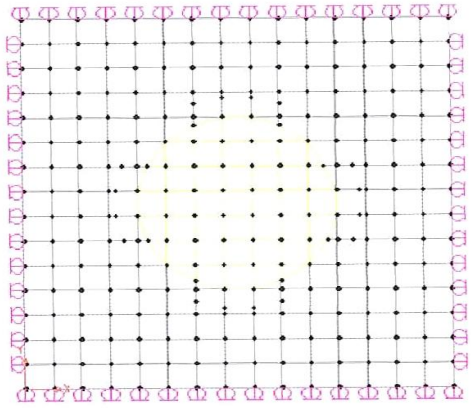

Figure 1. Finite element model, plan

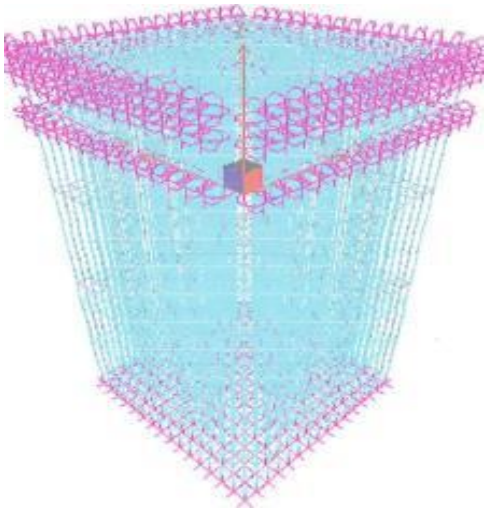

Figure 2. Finite element model, isometric

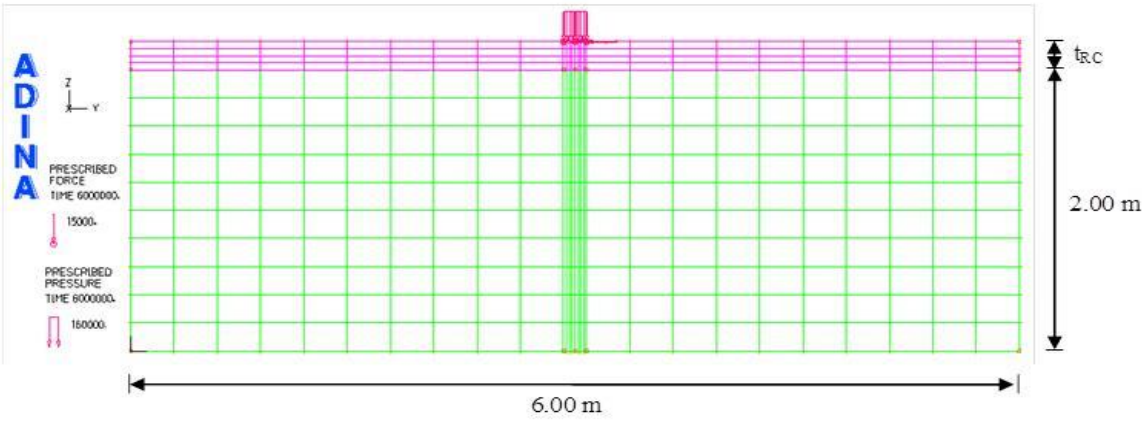

Figure 3. Problem definition of soil structure interaction

2. MATERIALS AND METHODS

Cement used was the Ordinary Portland cement, type produced by the Suez cement factory. Its chemical and physical characteristics satisfied the Egyptian Standard Specification (ESS 4756-1/2009) [3]. Fine aggregate used in the experimental program was natural siliceous sand. Its characteristics satisfy the Egyptian Code of Practices (ECP 203/2007) [4], (ESS 1109/2008) [5]. It was clean and nearly free from impurities with a specific gravity 2.6 t/m³ and a modulus of fineness 2.7. Super Plasticizer used was a high rang water reducer HRWR. It was used to improve the workability of the mix. The admixture used was produced by Sika Group under the commercial name of ASTM (Sikaviscocrete 20), It meets the requirements of ASTM C494 (type A and F) (20). The admixture is a brown liquid having a density of 1.18 kg/liter at room temperature. The amount of HRWR was 1.0 % of the cement weight.

The water was used; clean drinking fresh water free from impurities was used for mixing and curing the tested plates according to (ECP 203/2007) [4]. Reinforcing Materials (Reinforcing Meshes) are Polyethylene Meshes: Two types of Polyethylene meshes were used, which obtained from Al Shrouk Company of synthetic fibers namely CE121 and CE131. These types of meshes are made from high density polyethylene. "Geogrid" were used. Tables 1 and 2 show the properties and photos of these meshes.

TABLE 1: TECHNICAL SPECIFICATION OF POLYETHYLENE MESH (CE121)

Size of opening	12x12 mm	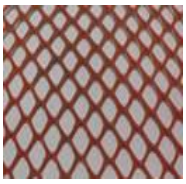
Thickness	3 mm	
Weight	529 g/m^2	
Tensile Strength	24.7 MPa	
Elongation in Long. Direction	21%	

TABLE 2: TECHNICAL SPECIFICATION OF TENSAR MESH

Size of opening	30 x 30mm	
Thickness	2mm	
Weight	200 g/m2	
Tensile Strength	260 MPa	
Elongation in Longitudinal Direction	20%	

3. METHODOLOGY:

Three dimensions FE models were prepared to study the response of airfield pavements at special runway sections where horizontal forces exist. The analysis model was established with a fixed boundary at the bottom and roller supports on sides, this confirms to the assumptions of Uddin *et al.* [16]. A single wheel load of 88000 lb was applied over a circular contact area of 68 cm diameter to represent the load of a wheel from the main gear of B-747. In addition to VL, HF was applied in the longitudinal direction to represent tractive or braking effort [17]. The value of this force varied depending on the coefficient of road adhesion (μ). The peak value of $\mu(\mu_p)$ ranges from 0.8 to 0.9 for dry asphalt concrete pavements and from 0.5 to 0.7 for wet asphalt pavements [13], But the allowable μ_p according to AASHTO is about 42 % in longitudinal direction [1], thus, the value of 0.45 were used as the coefficient of road adhesion in this study. This value resulted in a uniform pressure of 70 psi in longitudinal direction. Another HF may act in lateral direction due to camber thrust, centripetal force or any side force [17]. The peak value of this LTF equals to μ multiplied by VL, but the allowable μ_p is about 17% in lateral direction according to AASHTO [1]. Thus the coefficient of road adhesion in lateral direction was assumed equal to 0.2, this coefficient resulted in a uniform pressure of 31.4 psi in lateral direction.

Pavement structures were assumed to have three layers, the properties required for each layer were the thickness (h), Poisson's ratio (υ), and modulus of elasticity (E). The thickness of pavement layers were h_1 varied from 7.5 to 15 cm, h_2 = 25 cm, and h_3 = 240 cm such that the depth of the finite element model was taken ≥ four times the diameter of the wheel-pavement contact area to assure that stresses at this depth are insignificant. The Poisson's ratios were assumed to be υ_1 = 0.35, υ_2 = 0.30, and υ_3 = 0.40 for AC layer, base layer, and subgrade, respectively. Moduli of elasticity were assumed such that E_1 ranged from 500 to 3000 MPa, E2 = 250 MPa, and E_3 = 50 MPa for the three pavement layers, respectively. Table 3 summarizes layer properties data for all models under study.

3.1 RESPONSE OF AIRFIELD PAVEMENTS

Table 4 presents the maximum surface deflection (MSD) of pavement structure for different AC layer thickness and AC layer modulus under various loading conditions. The table shows that, there is a slight increase in MSD due to the existence of horizontal forces in addition

to the vertical aircraft wheel load. On the other hand, the thickness h_1 has a significant effect on MSD, as h_1 increases, MSD decreases considerably. The percentage of reduction in the MSD increases with higher E_1 values. Clearly, MSD decreases if better AC layer (with higher modulus of elasticity E_1) is used.

Figures 3-5 show the relationship between the maximum horizontal tensile strain at the bottom of AC layer st and AC layer thickness h_1 for different E_1 values of 500 MPa, 1500 MPa, and 3000 MPa, respectively. Clearly, ε_t, increases when horizontal forces exist at critical airfield sections. The differences in ε_t, values decrease as h_1 increases. In other words, the effect of horizontal forces on E_1 decreases as the AC layer thickness increases. The FE results showed a slight increase in ε_t values when loading case III is applied to the model compared to those when case II is applied. It means that the combination of horizontal forces in both longitudinal and lateral direction does not cause significant effect on the response of airfield pavements compared to the effect of horizontal force in one direction (case II). Figure 3 shows that, there is a so-called critical h_1 value before which the increase in hi results in an increase in ε_t, this can be explained by the high flexibility of thin AC layers. However this phenomenon seems to be diminished for higher E_1 values as shown in Figures 5-6. On the other hand Figures 3-5 there is an inverse relationship between ε_t and E_1, ε_t decreases significantly as E_1 increases. At the same time, it is worth to note that, the effect of horizontal forces on ε_t decreases for higher E_1 values.

Table 3. Layer Properties Data

Property	Layer		
	AC	Untreated Base	Subgrade
Thickness (cm)	7.5	25	240
	10		
	12.5		
	15		
Poisson's Ratio	0.35	0.30	0.40
Modulus (MPa)	500	250	5
	1500		
	3000		

Table 4. Maximum Surface Deflections

E_1 (MPa)	h_1 (cm)	Loading Condition		
		Case 1	Case 2	Case 3
500	7.5	1.507	1.513	1.516
	10.0	1.491	1.496	1.498
	12.5	1.477	1.484	1.486
	15.0	1.466	1.473	1.475
1500	7.5	1.473	1.478	1.478
	10.0	1.451	1.456	1.458
	12.5	1.432	1.436	1.436
	15.0	1.416	1.421	1.421
1500	7.5	1.454	1.458	1.460
	10.0	1.427	1.430	1.432
	12.5	1.403	1.407	1.408
	15.0	1.385	1.389	1.390

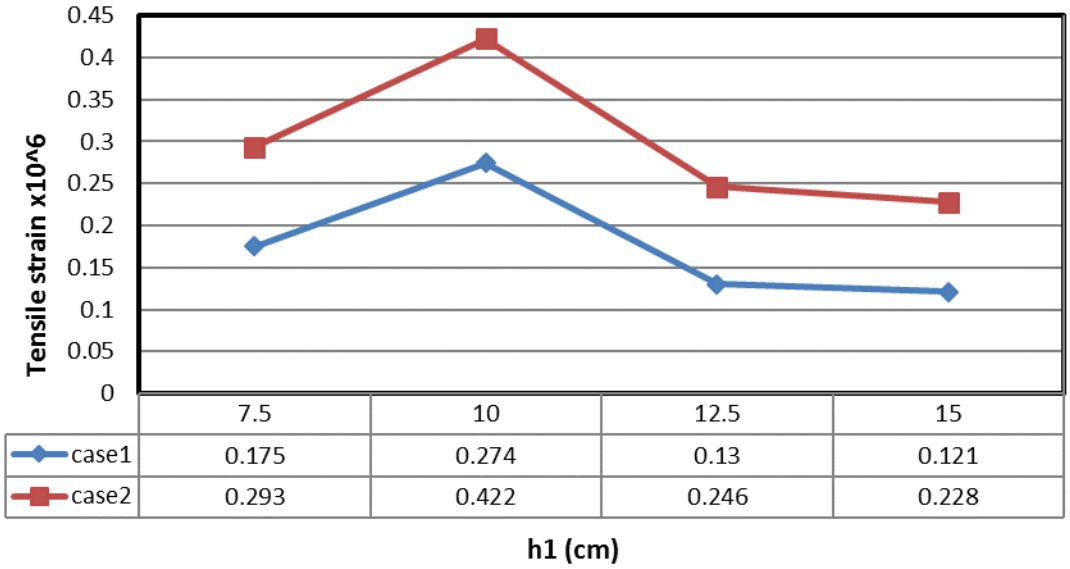

Figure 3. Tensile strains at bottom of AC layer versus AC thickness, E_1 = 500 MPa

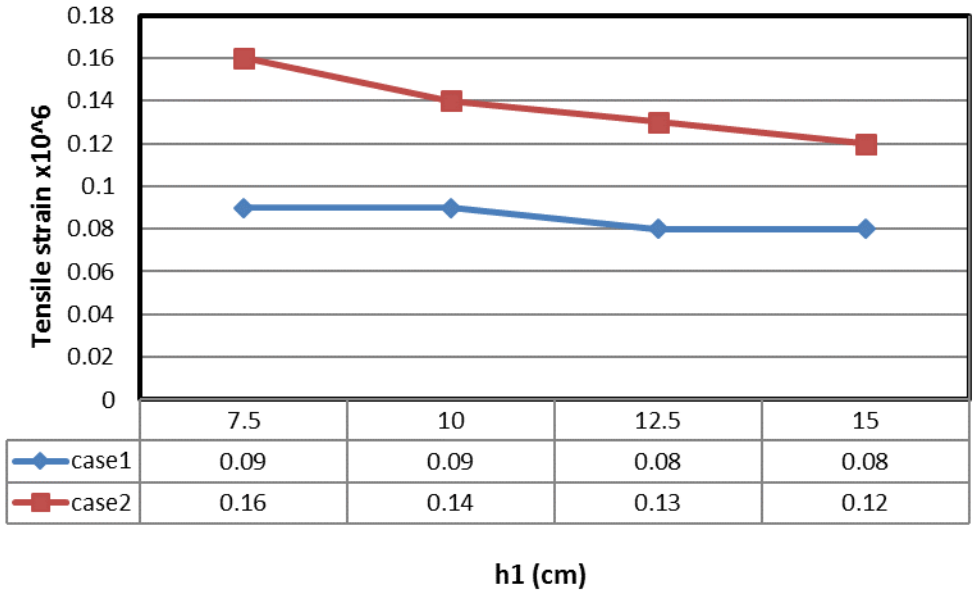

Figure 4. Tensile strains at bottom of AC layer versus AC thickness, E1 = 1500 MPa

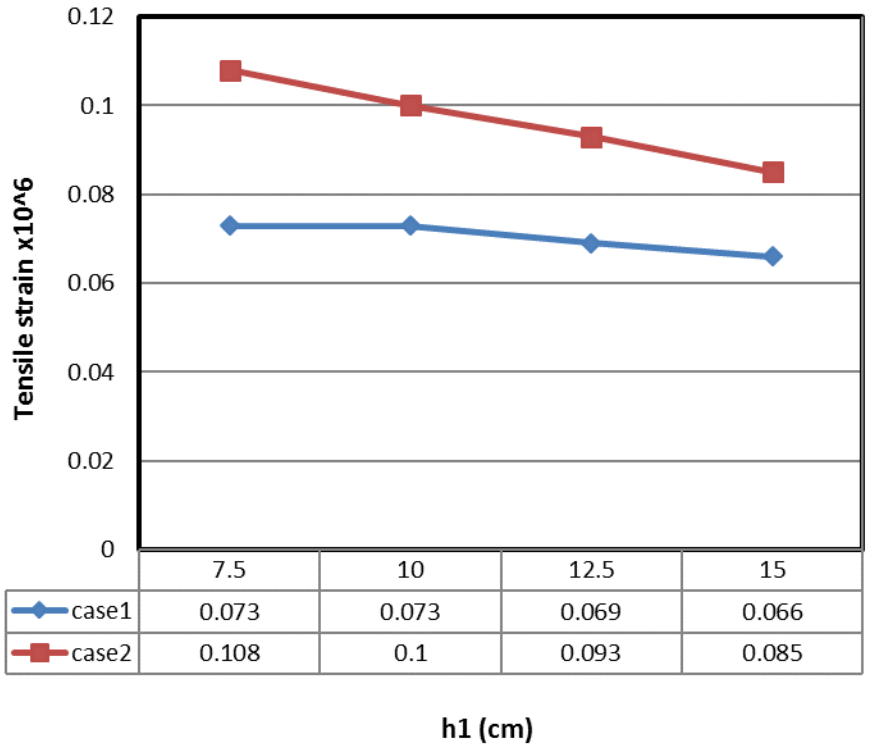

Figure 5. Tensile strains at bottom of AC layer versus AC thickness, E_1 = 3000 MPa

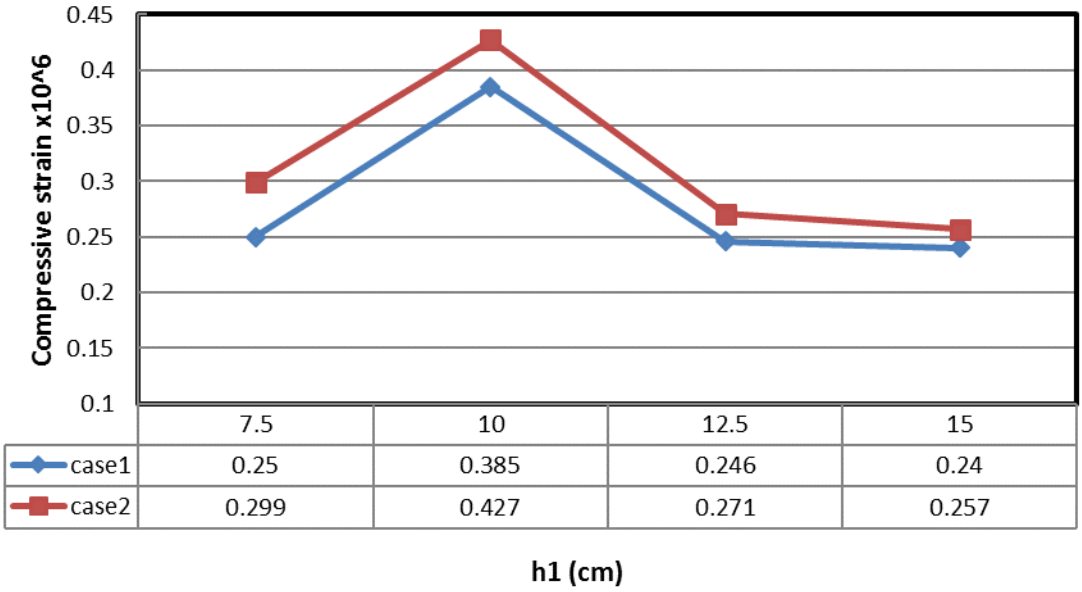

Figure 6. Compressive strains at top of subgrade versus AC thickness, E1 = 500 MPa

3.2. AIRFIELD PAVEMENT LIFE

Airfield pavement life is presented in this study as the minimum of allowable number of load repetitions till fatigue cracking (N_f) and allowable number of load repetitions to control permanent deformation (N_d). Based on st and ε_c pavement life was calculated as [15];

$$N_f = 0.0796\ \varepsilon_t^{-3'29\ t}\ E_1^{-0.854} \qquad (1)$$

$$N_d = 1.365 \times 10^{-9}\ \varepsilon_c^{-477} \qquad (2)$$

where:

N_f : allowable number of load repetitions before fatigue cracking.
ε_t : maximum horizontal tensile strain at bottom of asphalt concrete layer.
N_d : allowable number of load repetitions to control permanent deformation.
ε_c : maximum vertical compressive strain at top of subgrade.

It is noteworthy to mention that a small increase in ε_t or ε_c causes a considerable decrease in N_f and N_d, respectively. Table 5 presents the pavement life in terms of N_f and N_d for all cases under study. The table shows that, N_f and N_d decrease considerably when applying horizontal forces to the pavement structure (case II) compared to when applying vertical loads only as in case I.

The table shows also that case III does not yield considerable difference in N_f and N_d compared to case II. On the other hand, it was found that, N_f governs the airfield pavement life. As a result, pavement life in terms of N_f is showed against h_1 for E_1 of 500 MPa, 1500 MPa, and 3000 MPa. At critical airfield pavement sections, pavement life significantly decreases due to the presence of horizontal forces at these sections. The reduction in pavement life decreases as E_1 increases. Further reduction in the effect of horizontal forces on airfield pavement life can be obtained by increasing h_1.

Table 5. Airfield pavement life

E_1(MPa)	h_1 (cm)	N_f			N_d		
		Loading Condition			Loading Condition		
		Case 1	Case 2	Case 3	Case 1	Case 2	Case 3
500	7.5	7.33E+15	1.34E+15	1.28E+15	4.43E+20	1.99E+20	1.60E+20
	10.0	1.66E+15	4.03E+14	3.88E+14	6.45E+19	4.07E+19	3.54E+19
	12.5	1.96E+16	2.39E+15	2.26E+15	4.74E+20	3.07E+20	2.66E+20
	15.0	2.49E+16	3.05E+15	2.90E+15	5.34E+20	3.9E+20	3.49E+20
1500	7.5	5.52E+16	9.88E+15	9.88E+15	1.10E+22	5.22E+21	5.22E+21
	10.0	6.19E+16	1.5E+16	1.44E+16	8.75E+21	5.52E+21	4.81E+21
	12.5	7.18E+16	1.92E+16	1.92E+16	8.82E+21	6.64E+21	6.64E+21
	15.0	8.94E+16	2.43E+16	2.43E+16	1.01E+22	8.61E+21	8.61E+21
3000	7.5	7.2E+16	1.95E+16	1.89E+16	4.30E+22	2.54E+22	2.19E+22
	10.0	7.30E+16	2.55E+16	2.52E+16	3.73E+22	2.79E+22	2.55E+22
	12.5	8.72E+16	3.26E+16	3.23E+16	3.81E+22	3.49E+22	3.36E+22
	15.0	1.02E+17	4.37E+16	4.34E+16	4.52E+22	4.19E+22	4.04E+22

4. NEW MODEL ASSUMPTIONS:

The Employing New Innovative Material for Airfield Pavement static analysis are divided into two stages: Analysis Stage I (Static Loading Pattern): In this loading stage the soil is allowed to consolidate under its own weight, till the excess pore water pressure approaches zero, indicating the end of the consolidation stage. Analysis Stage II (Static Loading Pattern): In this stage the soil is loaded by the reinforced concrete layer own weight including excavating the soil.

4.1. USED NUMERICAL MODELS

Two dimensions FE models were prepared to study the response of airfield pavements at special runway sections where horizontal forces exist. The analysis model was established with a fixed boundary at the bottom and roller supports on sides, this conforms to the assumptions of Uddin *et al.* [16].

A single wheel load of 88000 lb was applied over a circular contact area of 16 cm diameter to represent the load of a wheel. In addition to VL, HF was applied in the longitudinal direction to represent tractive or braking effort. The value of this force varied is taken as the function of vertical force. This value resulted in a uniform pressure of 15000 Pa in longitudinal direction.

Mohr-Coulomb Formulation: The Mohr-coulomb model is used in Soil Structure Interaction (SSI) finite element models efficiently and simply to characterize the non-linear behavior of the soil under static or dynamic condition. The model is a two parameter model, mainly characterized by the well known soil shear strength parameters (c and φ), in addition to other well-known soil parameters, like the soil modulus (E), and the Poisson's ratio (υ). Soil angle of dilation (ψ) can be fed to the program considering a non-associated flow rule [2].

It should be noted that some advanced soil models have something like twenty parameters or so. Despite being very accurate when modeling the original problems they were calibrated for, these models usually fail in modeling any other geotechnical problem for simple reasons. First, the large number of model parameters rendered the model much complexity increasing the chance of errors in modeling. In addition, the real meaning of these parameters is not usually comprehended, even for simpler models like the Cam-Clay model [10].

Porous media formulation: The porous domain consists of both fluid and solid. The formulation of the porous media is applicable to porous structures subject to static or dynamic loading. It deals with the interaction between the porous solids and pore fluids, which flow through the porous solid skeleton as prospected in Figure 7.

In this study, a 2D plan strain solid element with 4-nodes, and displacement degrees of freedom at each node is used in the analysis. These elements have extra pore pressure nodes at their corner points [10].

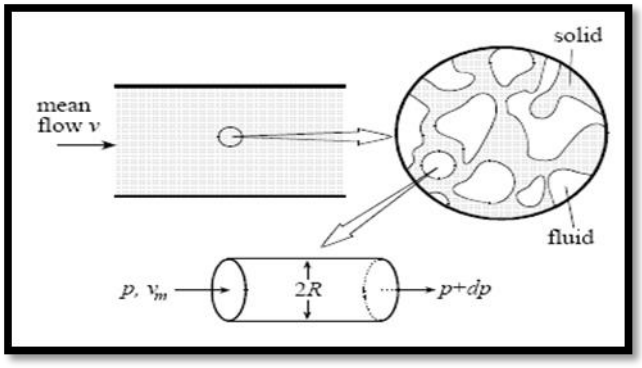

Figure 7. Illustration of porous media models.

Pavement structures were assumed to have two layers; natural medium stiff clay soil layer with parameter: density ρ = 1700 Kg/m^3, Cohesion, C= 22 KPa, Angle of internal friction (φ^o) = 1, Compressive modulus E= 1.5 MPa and Angle of Dilation (ψo) = 0.000001.

Linear Elastic Material Models: The linear isotropic material model is used to model the concrete in this research. These models are found in two material models; elastic-isotropic (isotropic linear elastic) and elastic-orthotropic (orthotropic linear elastic). These models can be employed using the small displacement or large displacement formulations. In all cases, the strains are assumed to remain small. When the elastic-isotropic and elastic-orthotropic materials are used with the small displacement formulation, the formulation is linear and when used with large displacement analysis, the total or the updated Lagrangian formulation is automatically selected by the program depending on which formulation is numerically more effective [2].

The reinforced concrete (RC) layer properties are taken as Elastic modulus (E) = 2.09*10^{10} Pa = 2.09 * 10^4 MPa, Poisson's ratio (υ) = 0.25 and Density of concrete (γ) = 2500 kg/m3. The thickness of pavement layers were h1 varied from 10, 15 and 20 cm respectively.

4.2. ANALYSIS OF THE RESULTS

Figure 8 shows the variation of vertical displacement with time. First, the vertical displacement is simply the decrease with time till the consolidation state. When the road layers construction starts, the vertical displacement mainly decrease due to removing layers of top soil, which quickly start to increase after the subgrade and RC layer are built in. These variations in vertical displacement with time are simulating actually what happen in the nature before any loads generated on the road. Figure 9 shows the variation of vertical displacement with concrete thickness (AC). Figures 10 and 11 show the variation of lateral displacement and Stress-ZZ distribution with concrete thickness respectively.

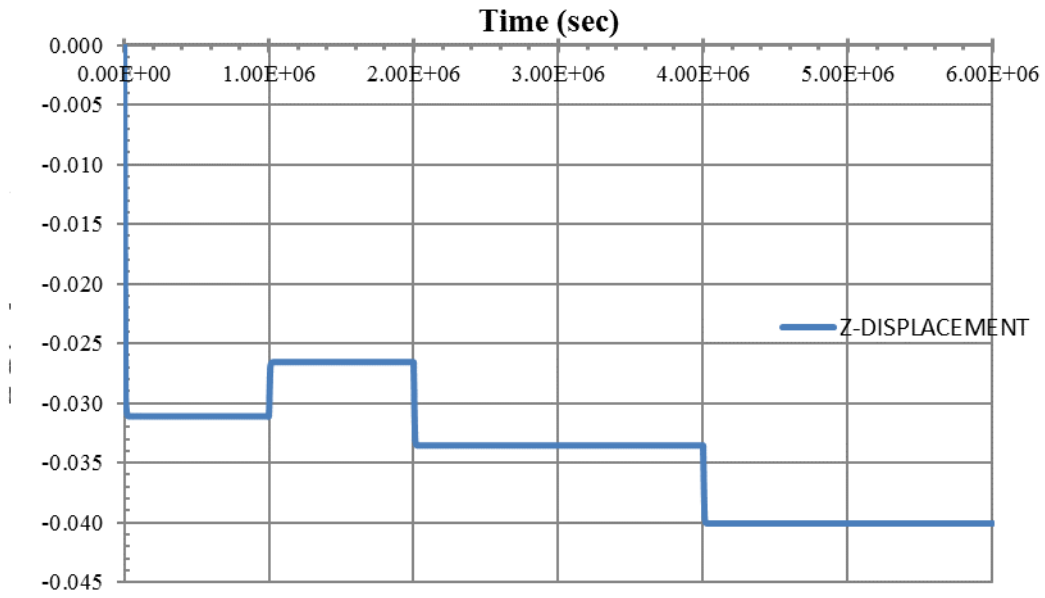

Figure 8. Vertical displacement along the time span at the interface between RC layer and the subgrade soil layer

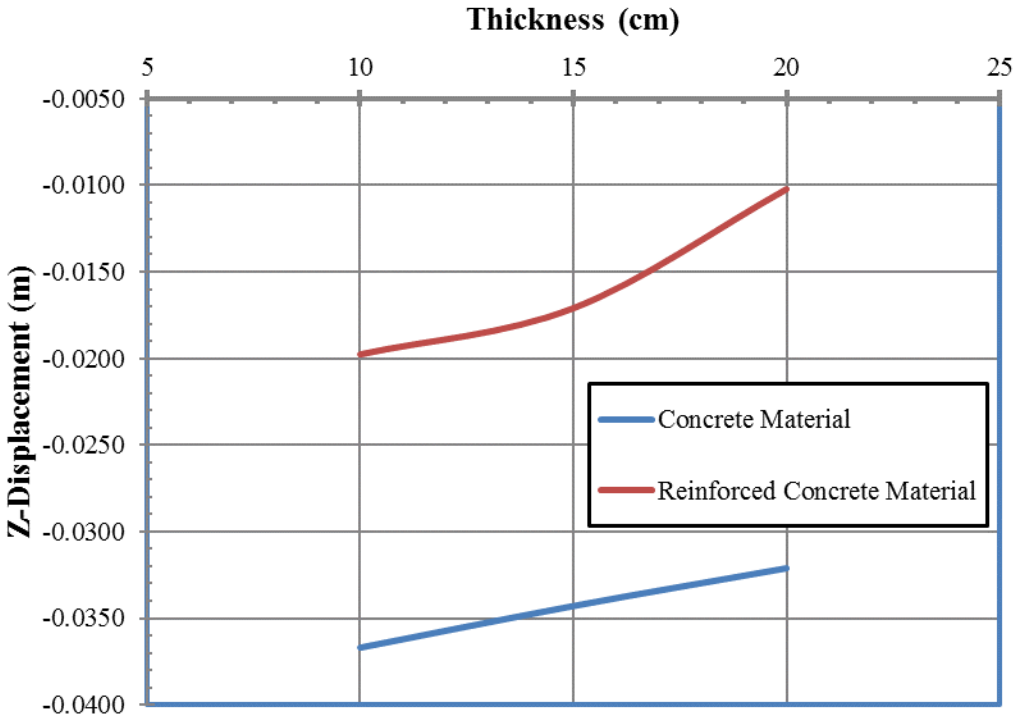

Figure 9. Vertical displacement distribution various concrete thickness.

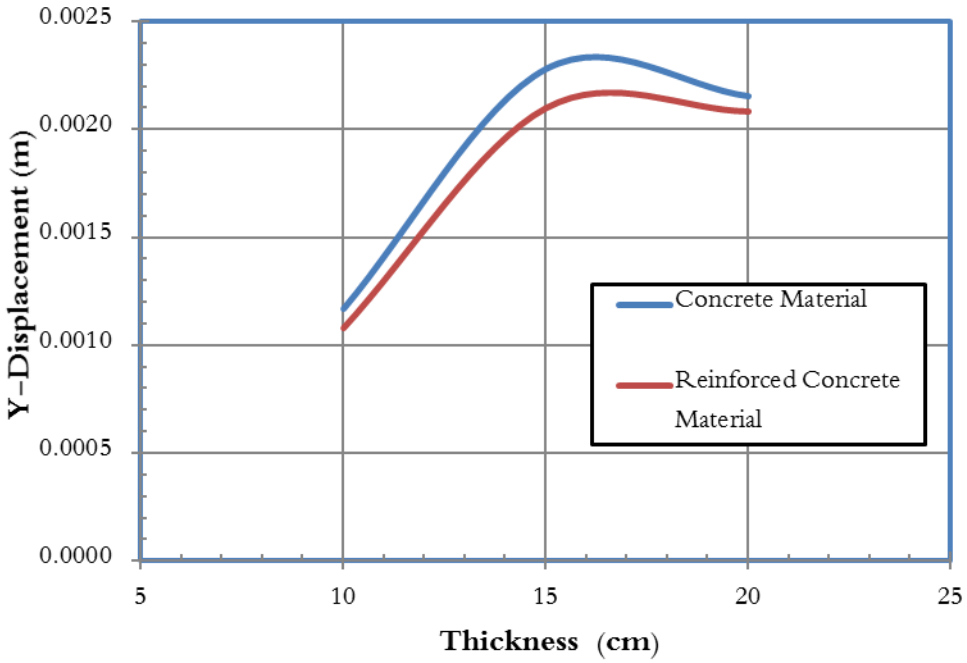

Figure 10. Lateral displacement distribution various concrete thickness.

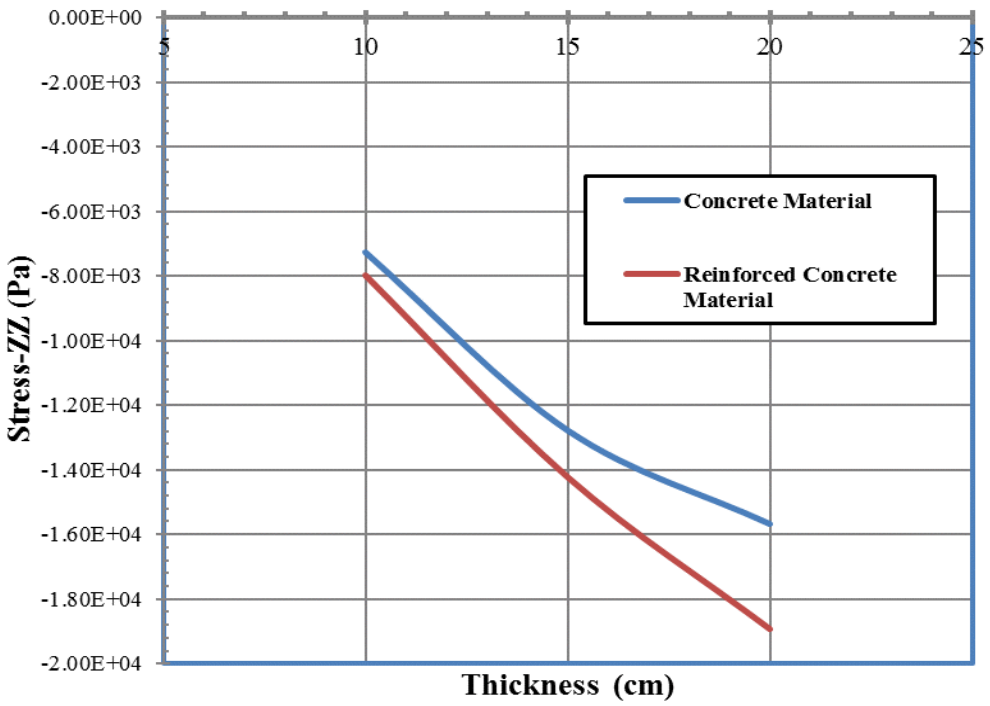

Figure 11. Stress-ZZ distribution various Reinforced concrete thickness.

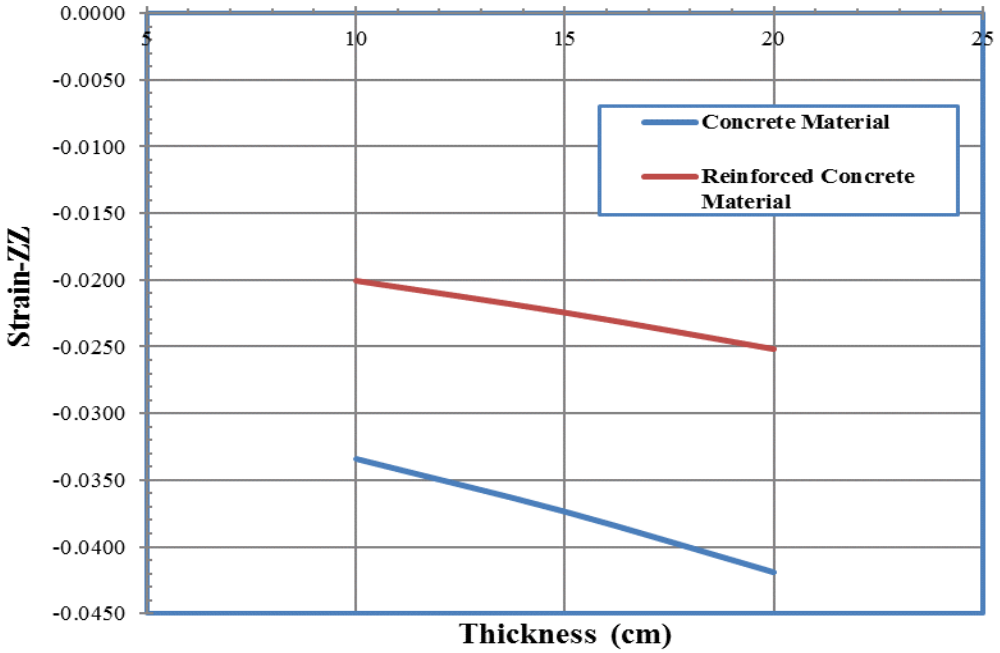

Figure 12. Strain-ZZ distribution various Reinforced concrete thickness.

5. CONCLUSIONS AND RECOMMENDATIONS

The vertical settlement depends mainly on the concrete thickness of the top layer. Under static loads, the settlement magnitude under the reinforced concrete layer is nearly less the settlement occurring under concrete without reinforcement by 20%. There is no significant effect of lateral displacement for concrete layer (AC) and reinforced concrete layer. The vertical stress on the reinforced concrete layer is approximately increased by about 15% than the concrete layer.

The tensile strain of the reinforced concrete layer is approximately decreased by about 17% than the concrete layer.

Linear models can be used to represent the relationship between pavement life and AC layer thickness. At critical airfield pavement sections, the pavement life decreases significantly due to existence of horizontal forces at these sections.

Using better AC material of higher elastic modulus can reduce the effect of horizontal sections on airfield pavement life. Further reduction of effect of horizontal force on airfield pavement life can be obtained by using reinforced concrete layer.

6. REFERENCES

1. AASHTO, "A Policy on Geometric Design of Highways and Streets," American Association of State Highway and Transportation Officials, Washington, D.C., (2004).
2. Bathe, K.J., (2011), "ADINA/Standard User's Manual, Version 8.7.3", Watertown, USA.
3. E.S.S. 4756-1/2009, 2009, Egyptian Standard Specification for Ordinary Portland Cement, Egypt.
4. E.C.P. 203/2007, 2007, Egyptian Code of Practice: Design and Construction for Reinforced Concrete Structures, Research Centre for Houses Building and Physical Planning, Cairo, Egypt.
5. E.S.S. 1109/2008, 2008, Egyptian Standard Specification for Aggregates, Egypt.
6. Huang, Y.H., 'pavement Analysis and Design. Prentice-Hall, Englewood Cliffs, N. I, (1993).
7. Mahmoud A. E.-W. and Kimio F. "Flexural Behavior of Lightweight Ferrocement Sandwich Composite Beams" Journal of Science& Technology, 2010, Vol. (15), No. (1), JST (3)
8. Monismith, C.L., "Analytically Based Asphalt Pavement Design and Rehabilitation," Theory to Practice, 1962-1992. In Transportation Research Record 1388, TRB, National Research Council, Washington, D. C., pp. 5-26, (1992).
9. Noor A. M., Salihuddin R. S. and Mahyuddin R. "Strength and Behaviour of Lightweight Ferrocement Aerated Concrete Sandwich Blocks" Malaysian Journal of Civil Engineering, (2006), 18(2): 99-108.
10. O'Neill, M.W., and Reese, L.C., (1999), "Drilled Shafts: Construction Procedures and Design Methods", FHWA-IF-99-025, Fedral Highway Administration, Washington, D.C., USA.
11. Salem, T.S., (1997), "Analysis of Offshore Piles", Ph. D. Thesis, Department of Structural Design, Zagazig University, Zagazig, Egypt.
12 Shaheen Y.B., Safan M.A., Abdalla M "Structural Behavior of Composite Reinforced Ferrocement Plates" Concrete Research Letters, Sept. 2012, Vol. 3 (3)
13. Taborek, J.J., "Mechanics of Vehicles," Machine Design, (2005).
14. The Asphalt Institute, "Thickness Design - Asphalt Pavements for Highways and Streets," Manual Series No. 1 (MS - 1), (1981).

15. Thompson, M. *et al.*, "Calibrated Mechanistic Structural Analysis Procedures for Pavement," NCHRP Report 1-26, Washington, D. C., (1992).
16. Uddin, W., Zhang, D., and Fernandez, F., "Finite Element Simulation of Pavement Discontinuities and Dynamic Load Response," Department of Civil Engineering, University of Mississippi, Miss. 38677. Transportation Research Record 1448, pp. 1 GO-106, (1994).
17. Wong, J.Y., "Theory of Ground Vehicles,"A Wiley- Inter-Science Publication, John Wiley& Sons, (1993).
18. Yue, Z.Q., and Svec, O.J., "Effects of Tire-Pavement Contact Pressure Distributions on The Response of Asphalt Concrete Pavements," Can. J. Civil. Eng. Vol. 22, (1995).